

$M\alpha/L\alpha$ Intensity Ratios for Ta, W, Pt, Au, Pb and Bi for Electron Energies in the 11–40 keV Range

J. Trincavelli,* S. Montoro,† P. Van Espen and R. Van Grieken

Department of Chemistry, University of Antwerp (UIA), B-2610 Antwerp-Wilrijk, Belgium

Both energy- and wavelength-dispersive systems were used to obtain $M\alpha/L\alpha$ intensity ratios for Ta, W, Pt, Au, Pb and Bi at various overvoltages. A table of these ratios corrected for matrix absorption and detector efficiency is presented, in addition to an interpolatory function of $M\alpha/L\alpha$ generated ratios vs. overvoltage, for each element. In addition, three different ZAF correction models were used to predict both detected and generated ratios. Finally, experimental $M\beta/M\alpha$ ratios measured at different overvoltages are presented for the six elements considered.

INTRODUCTION

Owing to the limited resolution of Si(Li) and Ge detectors, overlap between peaks of different elements is commonly observed in electron probe x-ray spectra. The calculation of the net area of the analytically important lines is seriously hampered by this fact. Most methods for spectrum evaluation rely on the *a priori* knowledge of the relative intensities of the characteristic lines. Peak overlap, such as S $K\alpha$ /Mo $L\alpha$, S $K\alpha$ /Pb $M\alpha$, Si $K\alpha$ /W $M\alpha$ and P $K\alpha$ /Au $M\alpha$, thus requires an accurate estimate of the intensity ratio between lines originating from different shells. These ratios are not constant but depend on experimental conditions such as detector efficiency, attenuation of x-rays in the sample and the overvoltage, U_0 , i.e. the ratio of the primary beam energy, E_0 , to the critical energy E_c , of the (sub)shell to be excited.

In this work, the $M\alpha/L\alpha$ intensity ratios were studied both theoretically and experimentally with the aim of predicting them under given experimental conditions. These predicted values can then be used in the evaluation of x-ray spectra.

EXPERIMENTAL

Both wavelength-dispersive (WD) and energy-dispersive (ED) x-ray spectra of pure Ta, W, Pt, Au, Pb and Bi were obtained using a JEOL-733 electron microprobe equipped with a Tracor ED system. The WD spectra were measured by means of a PET crystal and a scintillator detector and the ED spectra by means of a Si(Li) detector at a take-off angle of 40°. Spectra were acquired at overvoltages ranging from 1.07 to 3.04, calculated for each element considering the excitation

energy corresponding to the L_{III} subshell. The incident energies varied in the range 11–40 keV. The electron beam incidence was normal, at current intensities of 2 nA for ED spectra and from 100 to 620 nA for WD spectra.

In order to obtain the $M\alpha/L\alpha$ ratios, ED spectra were used and the background was subtracted by means of the AXIL¹ spectral analysis package. Because of the limited resolution of energy-dispersive systems, the $M\beta$ – $M\alpha$ doublets could not be resolved. WD spectra were acquired to obtain $M\beta/M\alpha$ ratios; with these values, $M\alpha$ intensities from the ED spectra were derived in order to calculate the $M\alpha/L\alpha$ ratios. For both ED and WD spectra, some of the measurements were taken several times; in these cases, the mean values were considered.

RESULTS

After dead-time correction and background subtraction, measured $M\beta/M\alpha$ intensity ratios were plotted against E_0 for each element and a linear behaviour was found. As can be seen from Fig. 1, the intercepts and slopes increase with increasing atomic number, and for the three heaviest elements considered the values are experimentally indistinguishable. Table 1 shows the coefficients given by fitted straight lines.

It is possible to predict the detected $M\alpha/L\alpha$ intensity ratios for a given element and overvoltage from the equation

$$\frac{I_M}{I_L} = \frac{(ZAF)_M \omega_M f_M \varepsilon_M}{(ZAF)_L \omega_L f_L \varepsilon_L} \quad (1)$$

where Z , A and F are the atomic number, absorption and fluorescence corrections, respectively, ω is the fluorescence yield,^{2,3} f is the line fraction⁴ (intensity of the considered line to all lines originating from a transition to the same subshell) and ε indicates the detector efficiency. The subscripts L and M correspond to $L\alpha$ and $M\alpha$ characteristic lines and to the subshells related to them, L_{III} and M_V .

* On leave from the Department of Physics, Universidad Nacional de Córdoba, Córdoba, Argentina.

† On leave from Centro Regional de Investigación y Desarrollo de Santa Fe, CONICET, Santa Fe, Argentina.

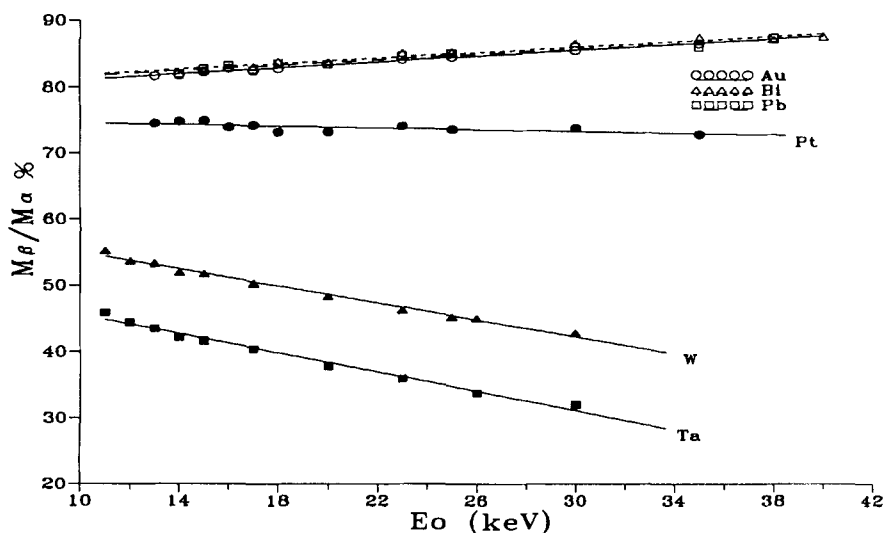


Figure 1. $M\beta/M\alpha$ intensity ratios for the six elements considered vs. incident electron energy E_0 .

The secondary vacancies in the M_V subshell were also included in the calculation of I_M . Thus, considering that, of the vacancies created in the L shell, only those originating in L_{III} can move to the M_V subshell, and taking into account that the fraction of L_{III} vacancies filled with M_V electrons is f_L , Z_M in Eqn (1) can be expressed as

$$Z_M = Z_M^1 + Z_L f_L \quad (2)$$

where Z_M^1 is the Z factor for primary M_V vacancies. The influence of this effect on the $M\alpha/L\alpha$ ratios was found not to be very important (only a few per cent for the highest overvoltages considered). For performing the atomic number and absorption corrections, three models were studied: the quadrilateral model of Sewell *et al.*⁵ and the Packwood and Brown Gaussian model⁶ as modified by Bastin *et al.*⁷ and as modified by Riveros *et al.*⁸ Fluorescence correction was not performed since it is negligible for pure element samples.

The detected $M\alpha/L\alpha$ ratios are strongly dependent on the matrix composition, mainly owing to the absorption in the sample, in contrast to the predicted $M\alpha/L\alpha$ ratios. The $M\alpha/L\alpha$ intensity ratios generated within the sample are expected to be less dependent on the composition since they are not affected by absorption; obviously, the

ratios are also independent of the detector efficiency. Hence the predicted ratios can be expressed as follows:

$$\frac{I_M}{I_L} = \frac{Z_M}{Z_L} \frac{\omega_M f_M}{\omega_L f_L} \quad (3)$$

In order to compare Eqn (3) with experimental data, measured $M\alpha/L\alpha$ intensity ratios were divided by the corresponding absorption correction. The model of Riveros *et al.*⁸ was chosen for performing the absorption correction, since this model fits experimental detected data slightly better than the other two, while all three models considered produced similar results for the absorption correction (the discrepancies between Rivero *et al.*'s model and the other two were always lower than 5% and only in 17% of the cases were they greater than 3%).

Figures 2–7 show a comparison between experimentally generated and predicted $M\alpha/L\alpha$ ratios for the six elements studied. The uncertainties in the experimental data (before correcting for absorption) range from 0.3% to 3%; the highest values correspond to the lowest overvoltages and drop rapidly with increasing U_0 . The smallest differences between experimental and predicted data correspond for $U_0 < 1.35$ for the quadrilateral model and for $U_0 > 1.35$ for Riveros *et al.*'s model. In both cases, typical discrepancies are around 20%, which are too large for quantitative analysis purposes. In order to produce a more reliable expression for predicted $M\alpha/L\alpha$ ratios, the following function of U_0 was fitted for each element:

$$\frac{I_M}{I_L} = a + b(U_0 - 1)^{-c} \quad (4)$$

Table 2 gives the values of the parameters a , b and c and the correlation coefficient, r^2 , corresponding to each fitting. Experimental $M\alpha/L\alpha$ ratios, corrected for absorption and detector efficiency, and $M\beta/M\alpha$ ratios, after dead-time correction and background subtraction, for all the energies and elements considered are given in Table 3.

Table 1. Slopes (a_1), intercepts (a_0) and their standard deviations (σ) for the straight lines fitted to experimental WD values of $M\beta/M\alpha$, in %, as a function of the incident electron energy, in keV (see Fig. 1)

Element	a_1	a_0	σa_1	σa_0
Ta	-0.72	52.8	0.03	0.6
W	-0.64	61.3	0.02	0.4
Pt	-0.06	75.2	0.02	0.5
Au	0.228	78.8	0.008	0.2
Pb	0.21	79.7	0.02	0.4
Bi	0.21	79.7	0.02	0.4

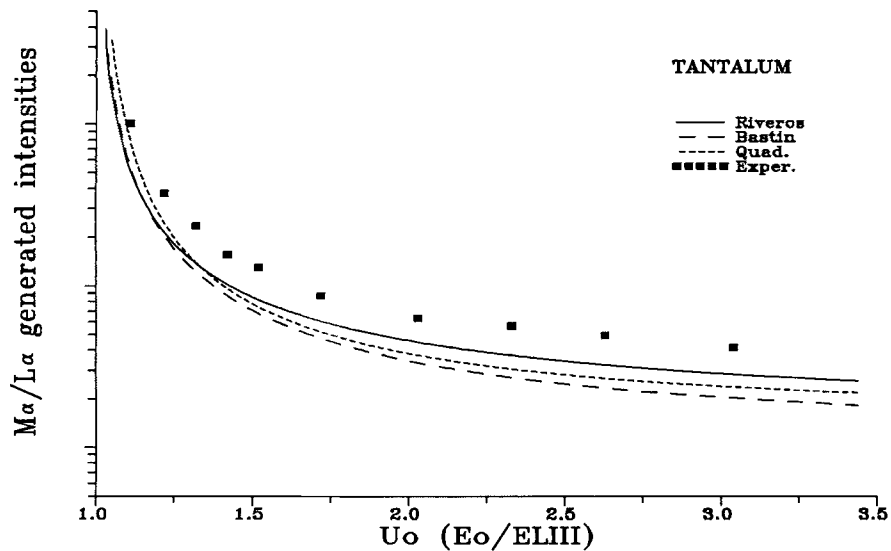


Figure 2. M_{α}/L_{α} generated intensity ratios for tantalum vs. overvoltage U_o with respect to L_{III} excitation energy. Absorption corrections given by Riveros *et al.*'s model applied to the experimental data. Solid line, Riveros *et al.*; long dashed line, Bastin *et al.*; short dashed line, quadrilateral model; ■, experimental.

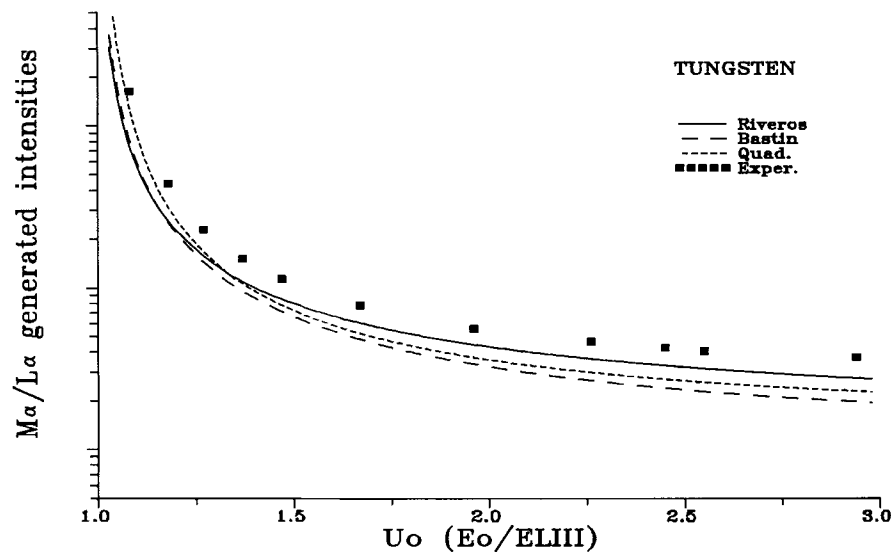


Figure 3. M_{α}/L_{α} generated intensity ratios for tungsten vs. overvoltage U_o with respect to L_{III} excitation energy. Absorption corrections given by Riveros *et al.*'s model applied to the experimental data. Identifications as in Fig. 2.

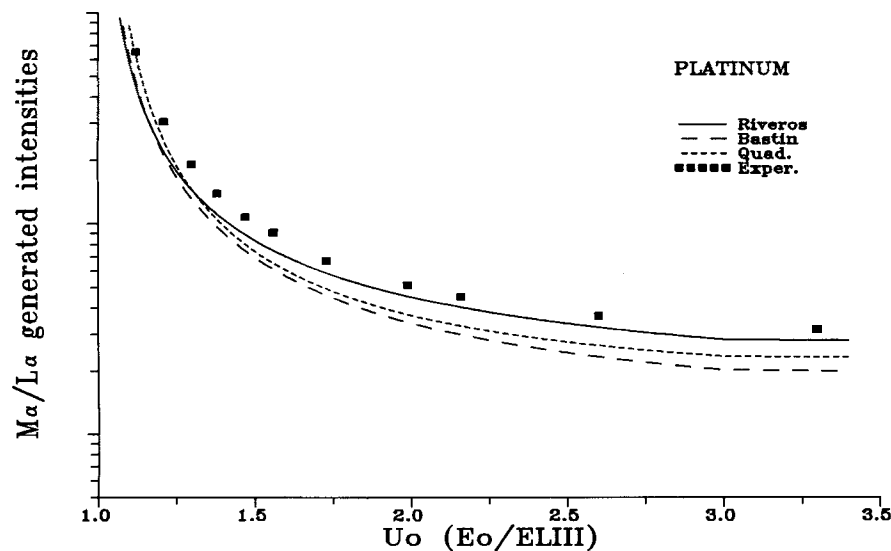


Figure 4. M_{α}/L_{α} generated intensity ratios for platinum vs. overvoltage U_o with respect to L_{III} excitation energy. Absorption corrections given by Riveros *et al.*'s model applied to the experimental data. Identifications as in Fig. 2.

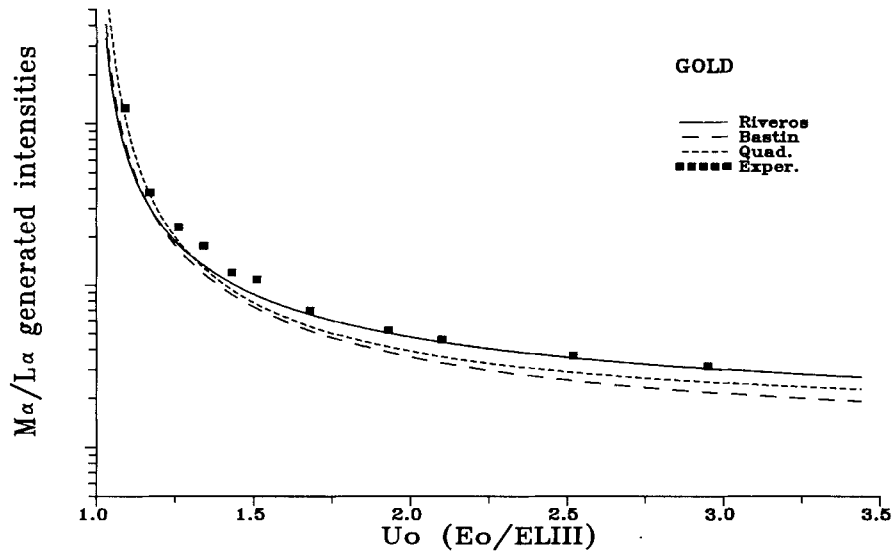


Figure 5. $M\alpha/L\alpha$ generated intensity ratios for gold vs. overvoltage U_o with respect to L_{III} excitation energy. Absorption corrections given by Riveros *et al.*'s model applied to the experimental data. Identifications as in Fig. 2.

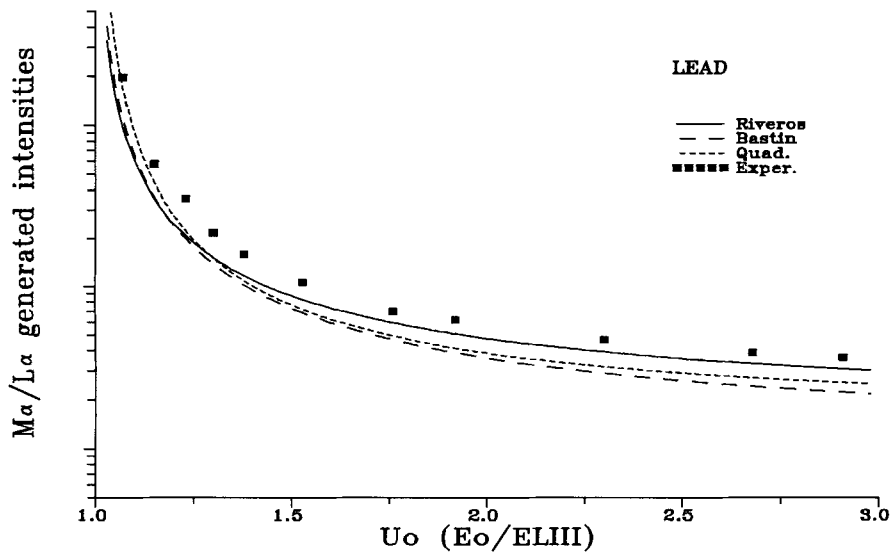


Figure 6. $M\alpha/L\alpha$ generated intensity ratios for lead vs. overvoltage U_o with respect to L_{III} excitation energy. Absorption corrections given by Riveros *et al.*'s model applied to the experimental data. Identifications as in Fig. 2.

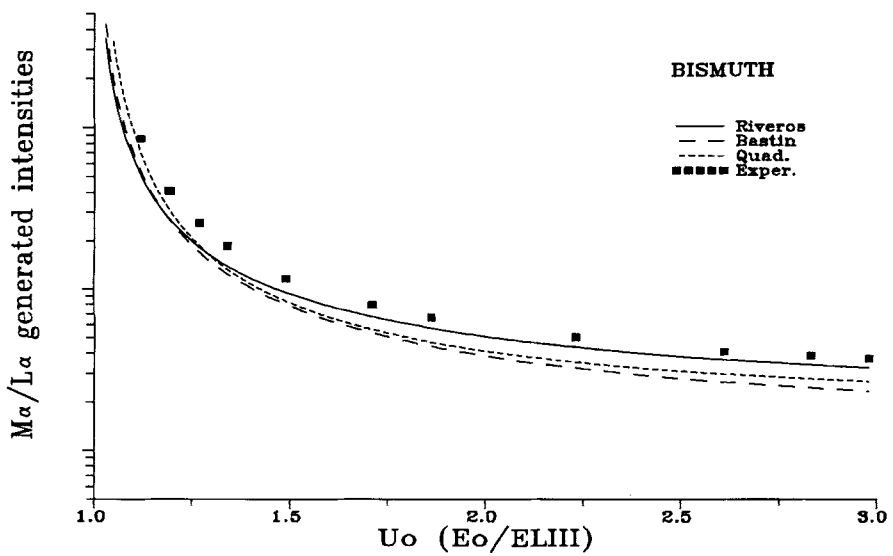


Figure 7. $M\alpha/L\alpha$ generated intensity ratios for bismuth vs. overvoltage U_o with respect to L_{III} excitation energy. Absorption corrections given by Riveros *et al.*'s model applied to the experimental data. Identifications as in Fig. 2.

Table 2. Coefficients for the function fitted to experimental ED values of $M\alpha/L\alpha$ (see Eqn (4))

Element	a	b	c	R^2
Ta	3.553	3.077	1.501	0.9998
W	2.223	3.110	1.691	0.99996
Pt	2.952	2.143	1.444	0.99995
Au	1.425	4.187	1.841	0.997
Pb	3.078	2.683	1.610	0.9994
Bi	3.072	2.643	1.620	0.9997

CONCLUSION

Both theoretical predictions and fitted curves allow $M\alpha/L\alpha$ values to be obtained over a wide range of experimental conditions. In the first case, the models could still be improved, especially with regard to the ionization cross-sections. (Bethe's model⁹ was used in

this work and there are a number of more recent models available.) The curves given by Eqn (3) and Table 2 fit the experimental data. These more realistic results will be used in a procedure for the evaluation of x-ray spectra based on non-linear least-squares fitting.¹

In addition, a linear relationship between $M\beta/M\alpha$ ratios and E_0 was found for all the elements considered; it would be of interest to extend the measurements to a larger set of elements in order to clarify the dependences of both $M\beta/M\alpha$ and $M\alpha/L\alpha$ on atomic number. A study of intensity ratios in binary or more complex samples would also be very helpful for studying matrix influences in $M\alpha/L\alpha$ detected and predicted ratios.

Acknowledgements

J. T. acknowledges financial support in the form of a scholarship from the Consejo Nacional de Investigaciones Científicas y Técnicas de la República Argentina. S. M. acknowledges scientific and financial support given by the University of Antwerp.

Table 3. $M\alpha/L\alpha$ experimental values corrected for absorption and detector efficiency and $M\beta/M\alpha$ experimental values after dead-time correction and background subtraction

E_0 (keV)	Ta		W		Pt		Au		Pb		Bi	
	$M\beta/M\alpha$	$M\alpha/L\alpha$	$M\beta/M\alpha$	$M\alpha/L\alpha$	$M\beta/M\alpha$	$M\alpha/L\alpha$	$M\beta/M\alpha$	$M\alpha/L\alpha$	$M\beta/M\alpha$	$M\alpha/L\alpha$	$M\beta/M\alpha$	$M\alpha/L\alpha$
11	45.9 ^a	100.62	55.2 ^a	162.52								
12	44.4 ^a	37.29 ^a	53.6	43.92								
13	43.5	23.37	53.3	22.73	74.5 ^a	65.12	81.7	124.57				
14	42.1	15.50 ^a	51.9 ^a	15.08	74.8	30.39	81.8 ^a	37.76	82.0	197.49		
15	41.6	12.95	51.7 ^a	11.32	74.9 ^a	19.07	82.3	22.88	82.8 ^a	57.40	82.5	85.26
16					73.9	13.89	82.8 ^a	17.42	83.3 ^a	35.19	82.9 ^a	40.94
17	40.4	8.67 ^a	50.3	7.79	74.2	10.72	82.5	11.92	82.6 ^a	21.67	83.1 ^a	25.74
18					73.2	9.05	82.8	10.80	83.7	15.80	83.9 ^a	18.52
20	37.8	6.31 ^a	48.3	5.57	73.2	6.68 ^a	83.5	6.95	83.4	10.59	83.8 ^a	11.61
23	35.9	5.62	46.3	4.64	74.1 ^a	5.14 ^a	84.2	5.24	84.8	6.98	85.2 ^a	7.92
25			45.2 ^a	4.27	73.6	4.51 ^a	84.6	4.59	85.2	6.18	85.3	6.63
26	33.7 ^a	4.92	45.0	4.06								
30	32.0 ^a	4.15 ^a	42.8	3.71	73.8 ^a	3.67 ^a	85.6 ^a	3.64	86.2	4.67	86.7 ^a	4.99
35					72.9	3.18 ^a	81.7	3.14	86.1 ^a	3.89	87.6	4.07
38									87.6	3.62	87.4	3.84
40											87.8 ^a	3.68

^a Averages of different measured values.

REFERENCES

1. P. Van Espen, K. Janssens and J. Nobels, *Chemometr. Intell. Lab. Syst.* **1**, 109 (1986).
2. J. Hubbell, *Report NISTIR 89-4144* (1989).
3. M. Chen and B. Crasemann, *Phys. Rev. A* **21**, 449 (1980).
4. J. Scofield, *Phys. Rev. A* **10**, 1507 (1974).
5. D. Sewell, G. Love and V. Scott, *J. Phys. D* **18**, 1245 (1985).
6. R. Packwood and J. Brown, *X-Ray Spectrom.* **10**, 138 (1981).
7. G. Bastin, H. Heijligers and J. Van Loo, *Scanning* **8**, 45 (1986).
8. J. Riveros, G. Castellano and J. Trincavelli, *Mikrochim. Acta, Suppl.* **12**, 99 (1992).
9. H. Bethe, *Ann. Phys.* **5**, 325 (1930).